COMITATO NAZIONALE PER L'ENERGIA NUCLEARE
Laboratori Nazionali di Frascati

LNF - 66/65
5 Dicembre 1966

C. Bacci, C. Mencuccini, G. Penso, A. Reale, G. Salvini, V. Silvestrini, M. Spinetti and B. Stella: PHOTOPRODUCTION OF NEUTRAL PIONS FOR INCIDENT PHOTON ENERGIES 400 ÷ 800 MeV. SEARCH FOR A RESONANT P_{11} STATE AND REMARKS ON THE γ CUSP EFFECT. -

(Nota interna: n. 340)

Servizio Documentazione
dei Laboratori Nazionali di Frascati del CNEN
Casella Postale 70 - Frascati (Roma)

Laboratori Nazionali di Frascati del CNEN
Servizio Documentazione

LNF-66/65

Nota Interna: n° 340
5 Dicembre 1966

C. Bacci(x), C. Mencuccini, G. Penso(x), A. Reale, G. Salvini(x), V. Silvestrini, M. Spinetti and B. Stella: PHOTOPRODUCTION OF NEUTRAL PIONS FOR INCIDENT PHOTON ENERGIES 400 ÷ 800 MeV. SEARCH FOR A RESONANT P_{11} STATE AND REMARKS ON THE η CUSP EFFECT. -

SUMMARY -

Photoproduction of neutral pions in the energy range $k \simeq 400$ to 800 MeV of the incident photon has been measured at the 1.1 Gev Frascati electronsynchrotron. The differential cross section as a function of energy at the π^0 c.m. angles $\theta^*_\pi = 90^\circ$, 120° and 135°, has been determined. The main feature of the experiment is a good resolution in the energy of the incident photon.

The results are compared with the existing theories in the energy range 450 to 550 Mev; the agreement is particularly good. All the cross sections exhibit a smooth behaviour as a function of energy for 400 Mev $< k <$ $<$ 600 Mev. No immediate evidence is found of a contribution of the P_{11} resonance. An anomaly seems to appear for $k \simeq 700 \div 740$ Mev, indicating a structure in the region of the so-called second resonance. The general behaviour of the cross section is examined taking into account the pion-nucleon scattering results. In particular, we try to interpret the observed anomaly as a reflection of the sharp opening of the η production channel (η cusp effect).

(x) - Istituto di Fisica dell'Università, Roma, and Istituto Nazionale di Fisica Nucleare, Sezione di Roma, Roma (Italy).

1) - INTRODUCTION -

The first attemps to give a phenomenological interpretation of the pion nucleon (π-N) interaction for a total c.m. energy E^* of the system smaller than $\sim$ 1800 Mev, were done mainly in terms of three resonant amplitudes: the three isobaric states P_{33} (1236 Mev), D_{13} (1518 Mev) and F_{15} (1688 Mev).

However, as the experimental material became more precise and the analysis more detailed, it turned out that this approach is certainly too naive.

The new experimental information came mainly from π-N scattering, to show that (see par. 5 and references quoted there):

a) - a P_{11} state, probably resonant, is present and important in the region between the first and the second resonance. Its contribution appears as a broad bump in the cross section for pion nucleon scattering and is clearly put in evidence in several detailed phase shifts analyses;

b) - other states than the mentioned ones are important at energies close to the second resonance: the relative importance of these states is however not yet known, large discrepancies being still present among the analyses of different authors.

The understanding of the π-N interaction in the concerned energy region is now waiting for new experimental data, from pion and photon beams.

In particular, the photoproduction data are rather scanty in the energy region between the first and the second resonance, and the measurements available around the second resonance have been performed, apart from few exceptions, with a rather poor energy resolution (see par. 5).

We describe in the following an experiment on π^o photoproduction

(1) $$\gamma + p \longrightarrow \pi^o + p$$

which has been performed at the 1.1 Gev Frascati electronsynchrotron, in order to contribute to the general information with some data collected with high energy resolution.

This paper is divided into six sections: in section 2 we describe the experimental lay-out; in section 3 the criteria used for data reduction; the experimental results are presented in section 4 and discussed in par. 5. In par. 6 we give our conclusions. In Appendix I we discuss some possible systematic errors; Appendix II, in connection with the discussion of par. 5, is devoted to some details on the calculation of a possible η-cusp effect.

2) - EXPERIMENTAL ARRANGEMENT -

The experimental lay-out is shown in fig. 1. It is the same used in an η-photoproduction experiment which has been described with some detail elsewhere(1). Some details on its use to detect the π^o photo production have been presented in ref. 2.

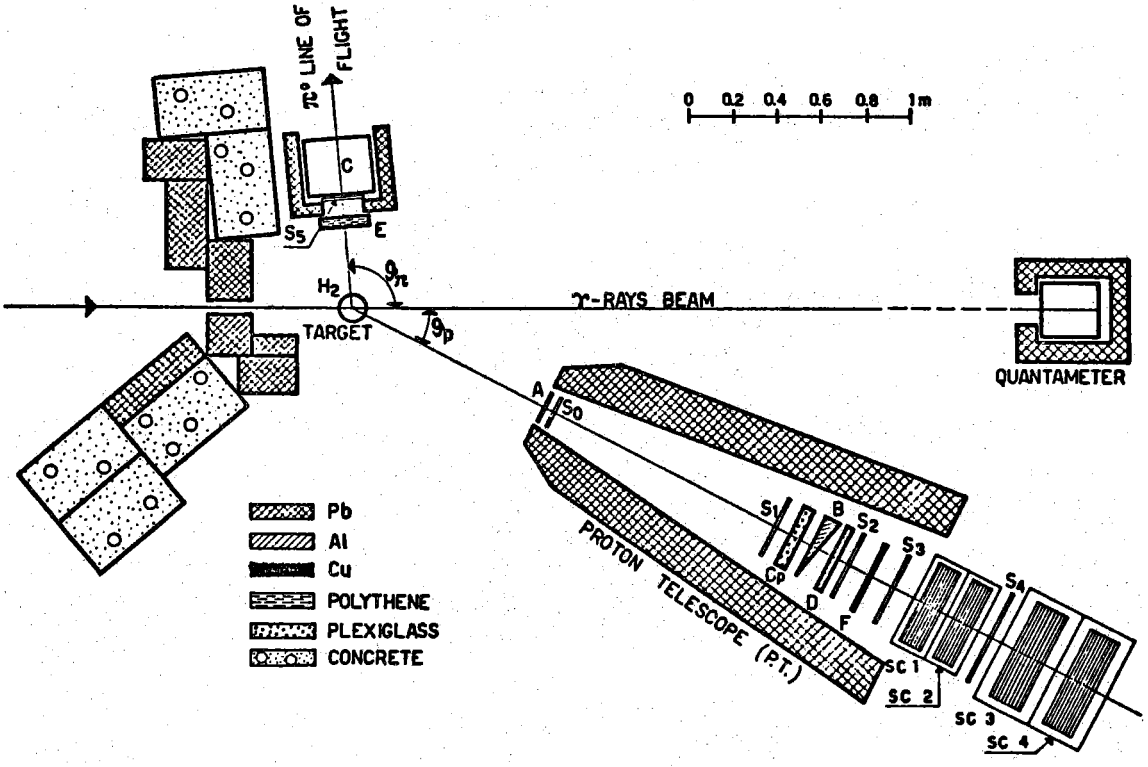

FIG. 1 - Experimental lay-out.

The γ-rays beam from the Frascati 1.1 Gev electronsynchro tron is incident upon a 7.4 cm liquid hydrogen target(3).

The proton telescope P. T. (fig. 1) consists in the scintillators S0 to S4, the plexiglass Cerenkov Counter Cp, and the four spark chambers SC 1 to SC4. In the spark chambers the angle and the range of the proton from reaction (1) are measured.

The γ-telescope consists of a total absorbtion lead glass Cerenkov counter C, with an anticoincidence scintillator S5 in front, to elimina te charged particles. The Cerenkov C detects γ-rays from the π^o's decay, and measures their energy through the pulse height. The polythène slab E shields S5 against low energy back-ground.

The spark chambers are triggered by a coincidence between a proton in the proton telescope and a photon in the γ-ray telescope. Discrimination against pions and electrons in the proton telescope is obtained by

use of the plexiglass Cerenkov counter Cp in anticoincidence, and of a pulse height discrimination on S1[2]. These criteria, (in addition to the request of a coincidence with a photon in C), reduce to 5-10% the contamination of relativistic particles in the triggers to the spark chambers. In addition, the pulse-heights in counters S2 and S3 are digitized and recorded on each photo. These informations allow complete elimination of pions and electrons when analyzing the data, as we shall see in next section.

The pulse height of Cerenkov C is also digitized and recorded on each photo.

The Cerenkov counter C has been calibrated by using monochromatic electrons from a pair spectrometer.

The block diagram of the electronics is shown in fig. 2. The beam intensity is monitored by a Wilson quantameter[4]. Since the counting rate in this experiment is rather high ($\sim$1 event per second = 1 event/20 machine pulses) and the advance of the film takes $\sim 1/3$ of a second, a substantial correction to the beam flux should be applied to correct for dead time. In order to reduce this effect, the synchrotron injection is antigated while the film is advancing. In this way the dead time effect is reduced to $\sim$5%, corresponding to events which are produced during the same machine pulse. We correct for this effect a posteriori.

The wedge shaped aluminum absorber B in the proton telescope (fig. 1) compensates approximately for the dependence of the energy of the recoil protons on their emission angle. A one to one correspondence between the range of the proton and the incident photon energy is thus obtained in most kinematical situations, symplifying the analysis of the data. When we thought it convenient, both informations (angle and energy of the proton) were used.

3) - DATA REDUCTION -

The first problem to be solved when analyzing the data, is to eliminate pions and electrons from the particles detected in the proton telescope. As we said, the electronics requirements on the triggers of the spark chambers already reduce to 5 ÷ 10% the contamination of relativistic particles.

The informations at our disposal to eliminate completely pions and electrons are:

- the range of the particle in the spark chambers;
- the pulse heights in counters S2 and S3.

For each set of particles whose range differs for less than

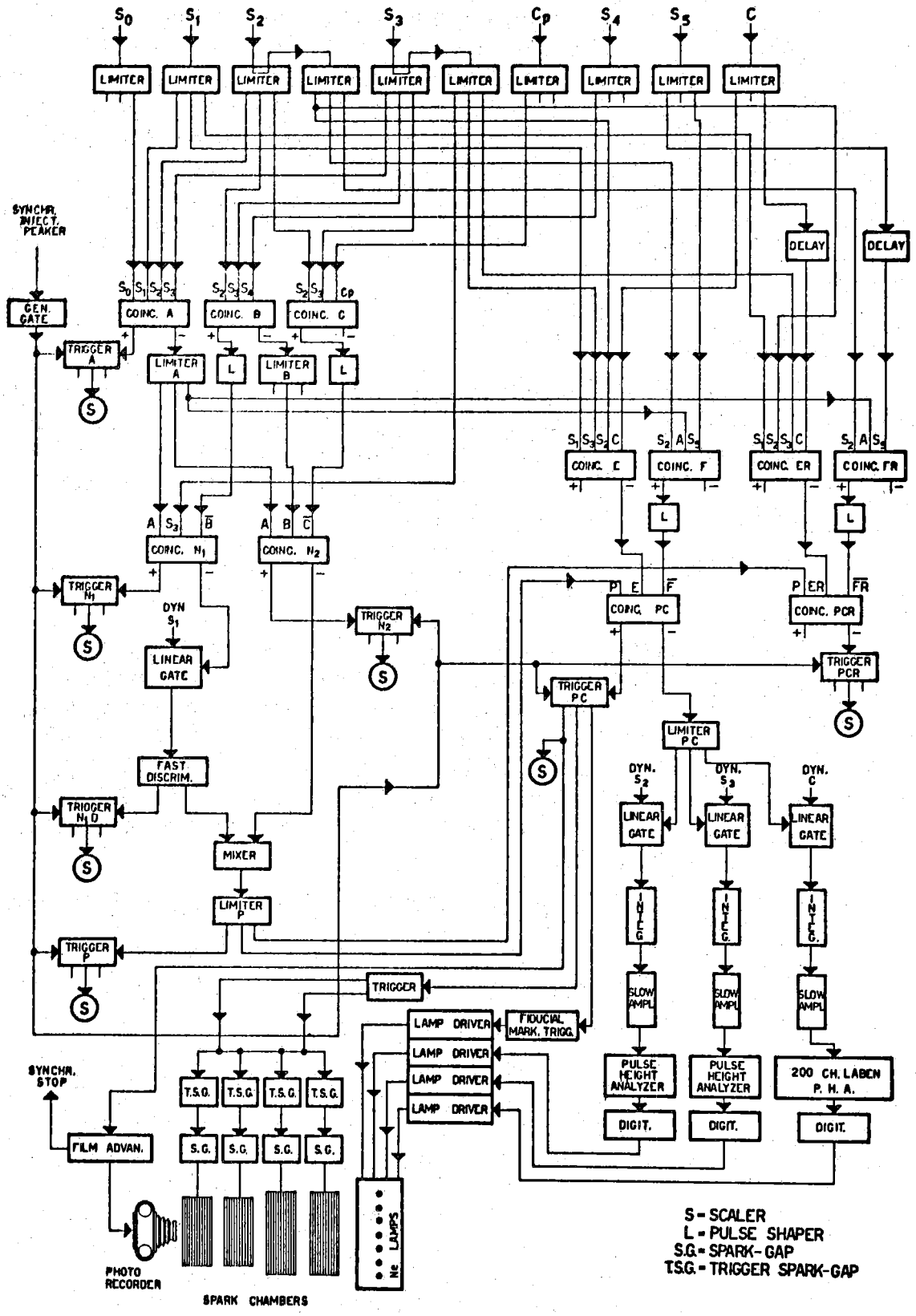

FIG. 2 - Block diagram of the electronics.

~ 2 gr/cm^2, we report in a two dimensional plot the pulse height distribution in counters S2 and S3. A typical bidimensional pulse height plot is shown in fig. 3: the number of pions in this sample has been increased for demonstration purposes by not requiring a coincidence with a γ-ray in C. Projecting this plot on the x x' axis of fig. 3, the pulse height distribution of fig. 4 is obtained. The elimination of relativistic particles can be performed in this way, with $\sim 1\%$ accuracy with respect to the number of protons.

Once pions and electrons have been eliminated, the accepted events are reported on a two dimensional plot in the variables proton range and photon energy in C.

A typical projection of such a plot on the proton range axis, is reported in fig. 5.

The spectrum obtained by projection on the proton range axis is strictly related to the cross section for process (1). In fact, apart from corrections discussed in the following, the shape of this distribution is an image of the spectrum of the incident bremsstrahlung beam, weighted by the cross section of reaction (1).

As a consequence, once the angle of the proton telescope is fixed, each set of our measurements (a set being defined by a particular choice of the machine energy and of the absorbers in the proton telescope) provides values of the cross section on a rather large range of k (100 ÷ 200 Mev). This point is important, since most systematic errors in the relative normalization of the points are avoided in this way. By changing the machine energy E_o (and possibly the absorbers in the P. T.) another interval of k is explored, which is generally chosen as to be partially overlapped with the previous one. The agreement between cross sections from two or more sets (figs. 9, 10, 11) in the overlapping region checks against possible normalization errors in different sets.

Once the proton spectrum has been obtained the following corrections are applied:

a) - Subtraction of empty target background and accidental rate: each of these corrections is of the order of 3 ÷ 5%.

b) - Correction due to nuclear interactions of the protons in the telescope and in the spark chambers. We use a mean free path of 110 gr/cm^2 as extracted from Millburn et al.[5]. The method used to apply this correction is described in detail in ref. 2. We take of course into account both the facts that the effective number of protons which would stop in a given spark chamber plate is lowered by the nuclear interactions in the preceeding absorber, and enhanced by the nuclear interactions in the considered plate, of the protons which would stop in the following plates. This correction is in some situation as high as 30% (in the highest energy points at $\theta^* = 135^o$).

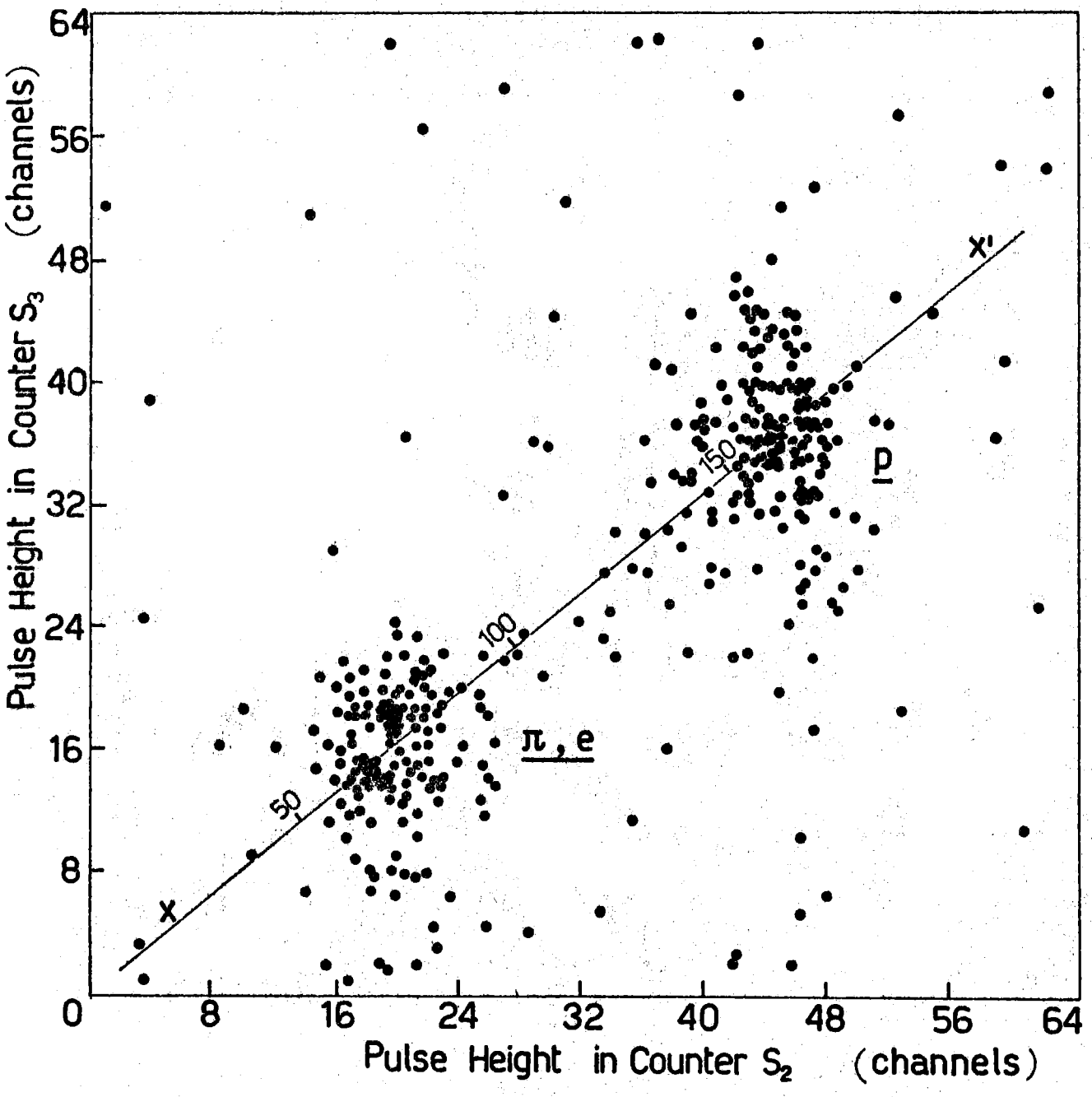

FIG. 3 - Bidimensional plot of pulse heights in counters S_2 and S_3. The number of pions and electrons has been increased for demonstration purpose by not requiring a γ-ray in coincidence with the proton.

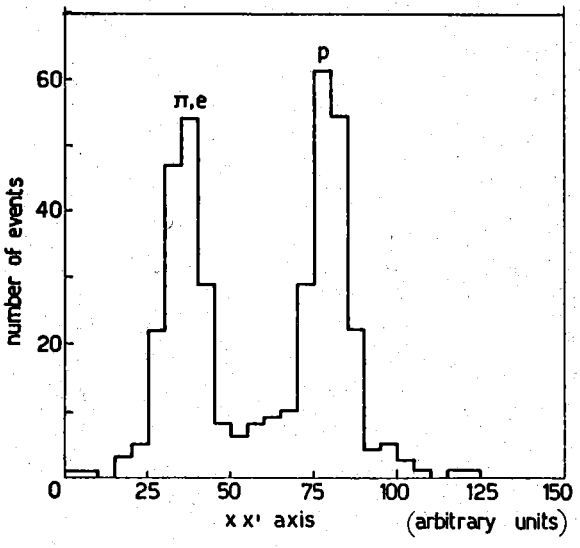

FIG. 4 - Distribution of fig. 3, projected on the x x' axis. Protons are clearly separated from the relativistic particles.

c) - Correction due to the efficiency of detection of the π^o by C. The geometrical efficiency has been evaluated by means of a Montecarlo calculation[2], and it is typically 40 ÷ 60% (fig. 6). Another effect we have taken into account is the possibility that a π^o is not detected by the electronics, if it gives a too small pulse height in C: in fact, if the electronics threshold on C is set too low, the accidental rate increases rapidly. We have set this threshold at a photon energy of ~80 Mev. To determine the correction for π^o's lost due to this threshold, we have plotted the pulse height distribution on C for photons in coincidence with protons belonging to small range intervals. A typical spectrum of this kind is shown in fig. 7. Depending on the kinematical situation, this correction goes from ~(5 ± 3)% to ~(10 ± 6)% (see Appendix I).

d) - Losses due to multiple scattering in the telescope. This effect has been computed and turned out to be negligible in our geometry. A check of this can be obtained by plotting the events as a function of their entrance point in the spark chambers. A rectangular distribution has been obtained (fig. 8), which is the shadow from the H_2 target of counter S3, which defines the solid angle. This plot checks also against counter misalignements.

e) - Contamination from multipion production. Once the proton telescope has been set at an angle θ_p, the energy k of the photon which produces reaction (1) is uniquely related with the energy of the proton detected in the telescope. By properly choosing the absorbers in the proton telescope and the machine energy E_o, it is possible to select k in such a way that

$$(E_o - 100 \text{ Mev}) \leq k \leq E_o \qquad (2)$$

This energy region is kinematically free from multipion production. Unless the energy distribution of protons from multipion production is strongly peaked towards the high energies, it is to be expected that the region free from multipion production extends to values of k somewhat smaller than indicated by relation (2). Our data with $\theta_{\pi}^{*} = 120^o$ and $\theta_{\pi}^{*} = 135^o$ were collected in many sets of measurements: the value E_o and the absorbers in the P. T. were set in such a way as to satisfy, in each measurement, relation (2), except for the points at lower energy in each set,

which are however superimposed to points from another measurement which satisfy relation (2). The comparison between the results of the different measurements (figs. 9 and 10) allow to conclude that the contamination from multipion production is, if any, very small (of the order of a few per cent).

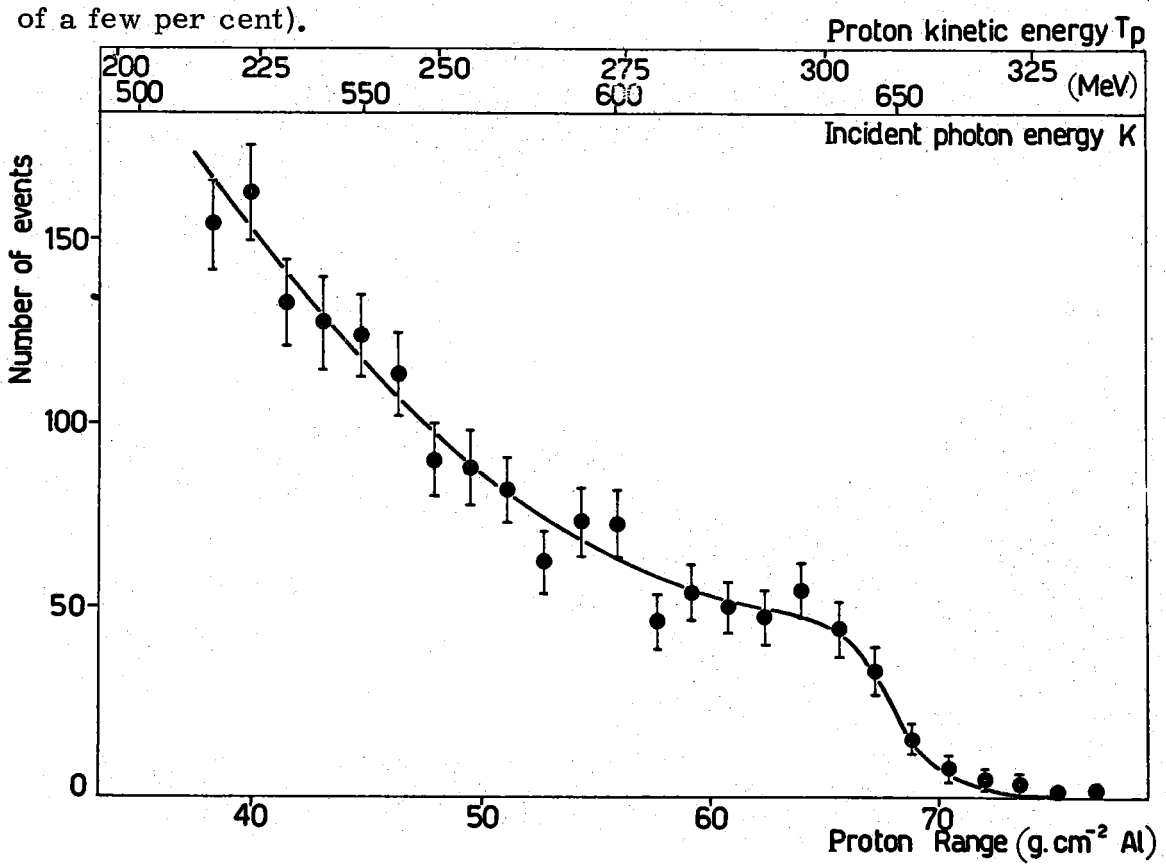

FIG. 5 - A proton spectrum as a function of the range. The kinetic energy of the proton and the energy of the photon producing reaction (1) are also reported (upper scales). The energy E_o of the synchrotron was 650 Mev, and in correspondence a step in the proton spectrum appears.

The data with $\theta_\pi^* = 90^o$ were collected in two sets of measurements, with E_o = 850 Mev and E_o = 750 Mev (fig. 11). Contamination from multipion production could thus be present in the first set for $k < 750$ Mev and in the second for $k < 650$ Mev, giving therefore at low energy, higher cross sections for the set with E_o = 850 Mev. However, since the data collected with E_o = 750 Mev are at low energy if any higher than the data with E_o = 850 Mev, (the two sets being however consistent within statistics), we considered negligible also in this case the contribution from multipion production.

f) - Contribution of the Compton effect on protons. A correction should be applied to our data in order to take into account the contamination from the elastic scattering of photons:

(3) $\gamma + p \longrightarrow \gamma + p$

This process is very hardly distinguishable from reaction (1), since the kinematics of the two reactions are very similar. However, the cross section for process (3) is of the order of 2%[6, 7] of the cross section for process (1). Since the efficiency of our Cerenkov counter to detect the γ-ray from process (3) is $\sim 100\%$, while the efficiency of detection of a γ-ray from process (1) is $\sim 50\%$, there is in our results a contamination of $\sim 4\%$ from process (3). We have not attempted to separate this contamination.

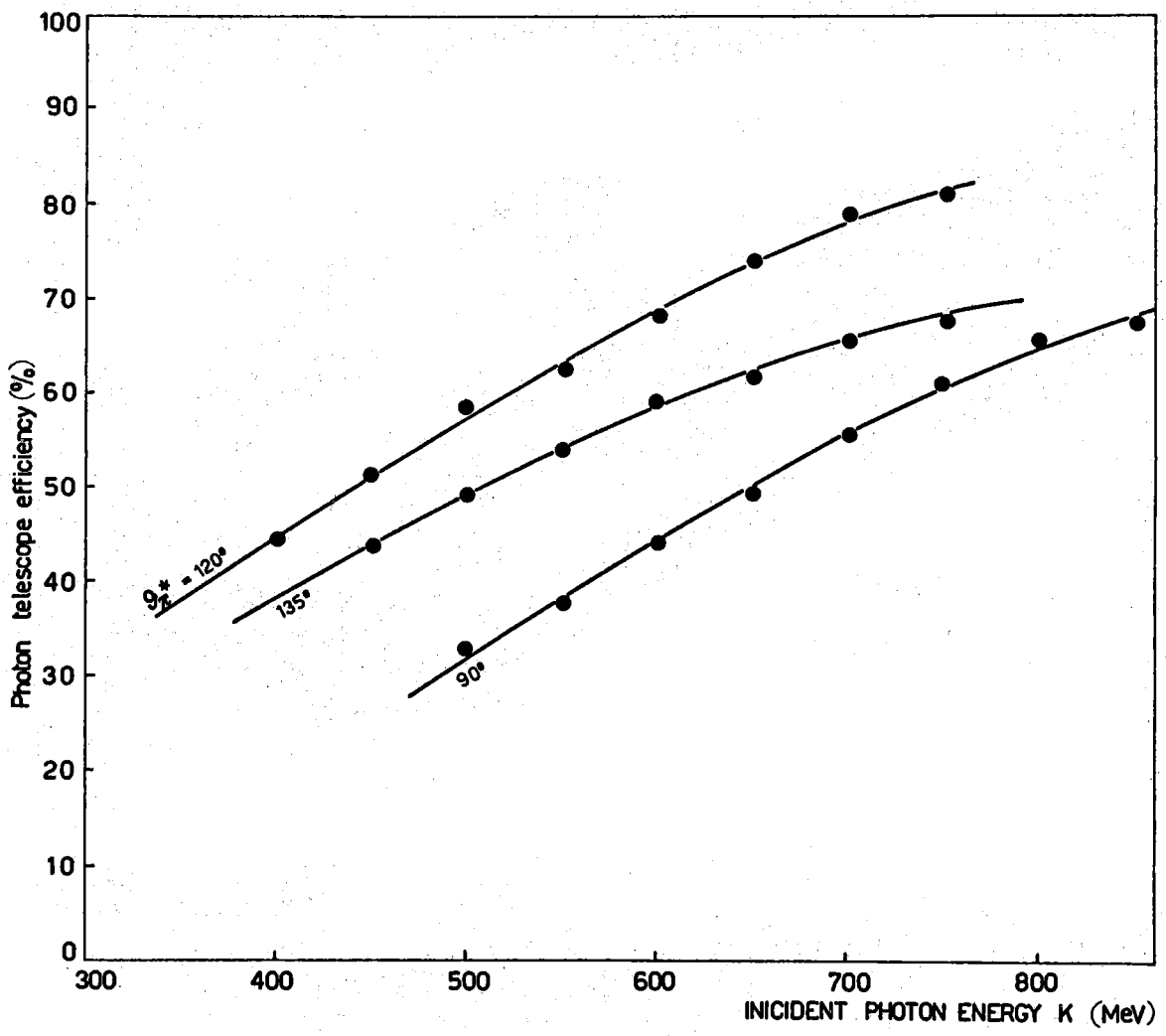

FIG. 6 - Cerenkov counter geometrical efficiency of π^0 detection, as obtained by a Montecarlo calculation. The three curves refer to the three kinematical situations chosen for this experiment. The distance from the H_2 target to the Cerenkov counter C was not the same at the three angles.

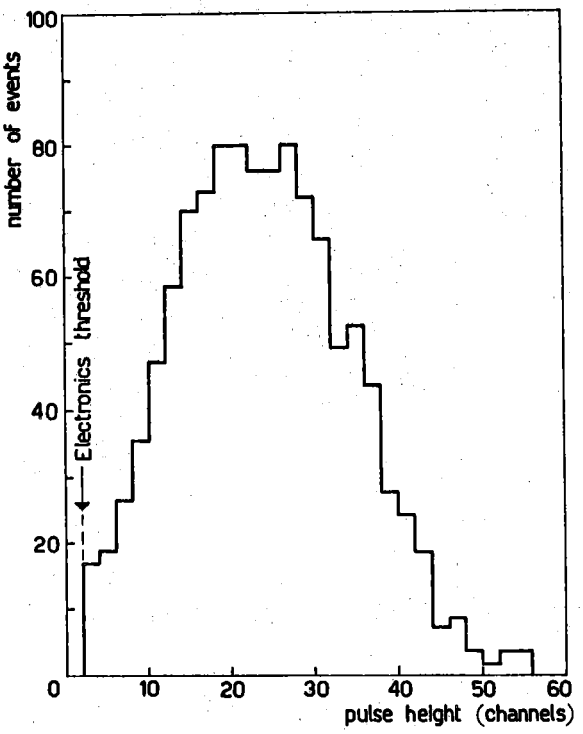

FIG. 7 - Pulse height distribution in C of the photons in coincidence with the protons in a small range interval. The number of events which are lost due to the electronics threshold on C is typically 5 ÷ 10%.

g) - Dead time corrections. As we said, most part of this correction is automatically done by stopping the synchrotron while the film is advancing. However, if two good events are produced by same machine pulse, the second one is lost. A correction for this effect is applied to the data, by comparing the number of photos with the number of events recorded on a scaler. This correction is of the order of 5%.

h) - Photos containing two tracks, or for some other reason not completely measurable, were disregarded at the scanning table. A correction for this effect (~ 2%) was applied to the final data.

i) - In connection with our conclusions (compare par. 5), some points of the measurement at $\theta_\pi^* = 90^\circ$ (the ones between k = 680 Mev and k = 750 Mev) are of particular importance. For this reason these data were handled with particular care. The scanning was performed three times independently by different scanners, obtaining consistent results and a correction was applied for the efficiency of the single gaps.

Once all these corrections have been applied to the experimental data, the corrected plot of the number of events vs. proton range is obtained. This plot is transformed into a plot $N(T_p)$ of the number of events vs. proton kinetic energy T_p. The cross section for process (1) is then obtained through the relation

$$\frac{d\sigma}{d\Omega^*} = \frac{N(T_p)(dT_p/dk)}{\frac{(b(k/E_o)}{k} \cdot \frac{d\Omega^*}{d\Omega} \cdot \Delta\Omega \cdot n \cdot Q}$$

where:

T_p : kinetic energy of the proton

k : energy of the incident photon

$N(T_p)$: number of events per unit interval of T_p

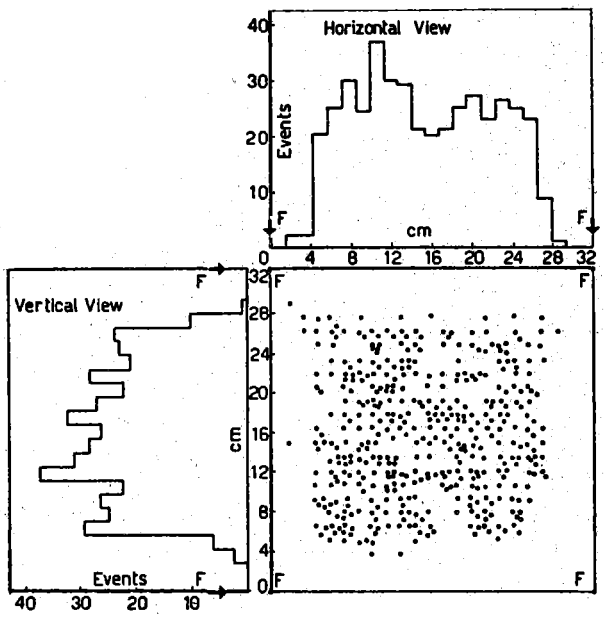

FIG. 8 - Distribution of the protons entering S.C.1 as a function of the entrance coordinates. This distribution fits well the shadow from the H_2 target of counter S_3, defining the solid angle. The fiducial marks F indicate the useful area of the spark chambers.

Q : number of equivalent quanta used to collect the data, as measured by the Wilson quantameter

$b(k/E_o)/k$: shape of the bremsstrahlung spectrum. The Bethe-Heitler formula has been used, corrected for the thickness of the internal target

n : number of atoms/cm^2 of the H_2 target

$\Delta\Omega$: solid angle of our proton telescope (6.7 msr).

4) - EXPERIMENTAL RESULTS -

The experimental results are presented in figs. 9, 10, 11, 12, 13 and 14. In figs. 9, 10, 11 the results of sets of measurements performed at different values of the machine energy E_o, are presented separately: the consistency among them is good.

In figs. 12, 13 and 14 and tables I, II and III our results are reported, after averaging according to the Crawford's procedure[8] on the different sets of measurements which were presented separately in figs. 9, 10 and 11.

The errors are only statistical. In fact the systematic errors we could think of, have a smooth behaviour as a function of energy; they cannot raise or destroy any possible "fine structure" effects, but affect the absolute normalization of our results. These errors will be discussed in Appendix I.

Our discussion of the possible presence of resonance or fine structures, will be based on the results and errors presented in figs. 12, 13 and 14. In the same figures, our resolution in the energy of the incident photon is also indicated.

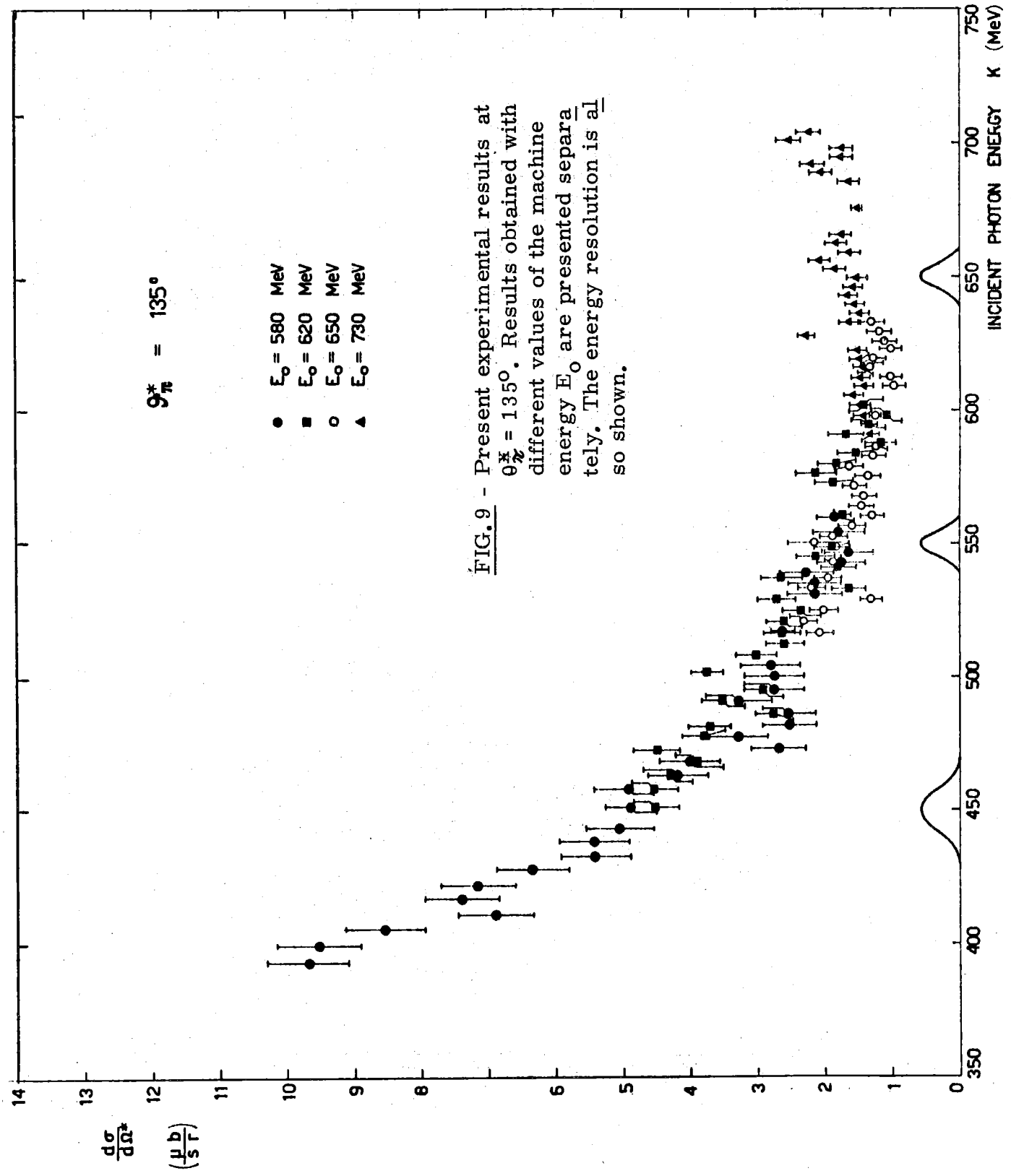

FIG. 9 - Present experimental results at θ^*_π = 135°. Results obtained with different values of the machine energy E_o are presented separately. The energy resolution is also shown.

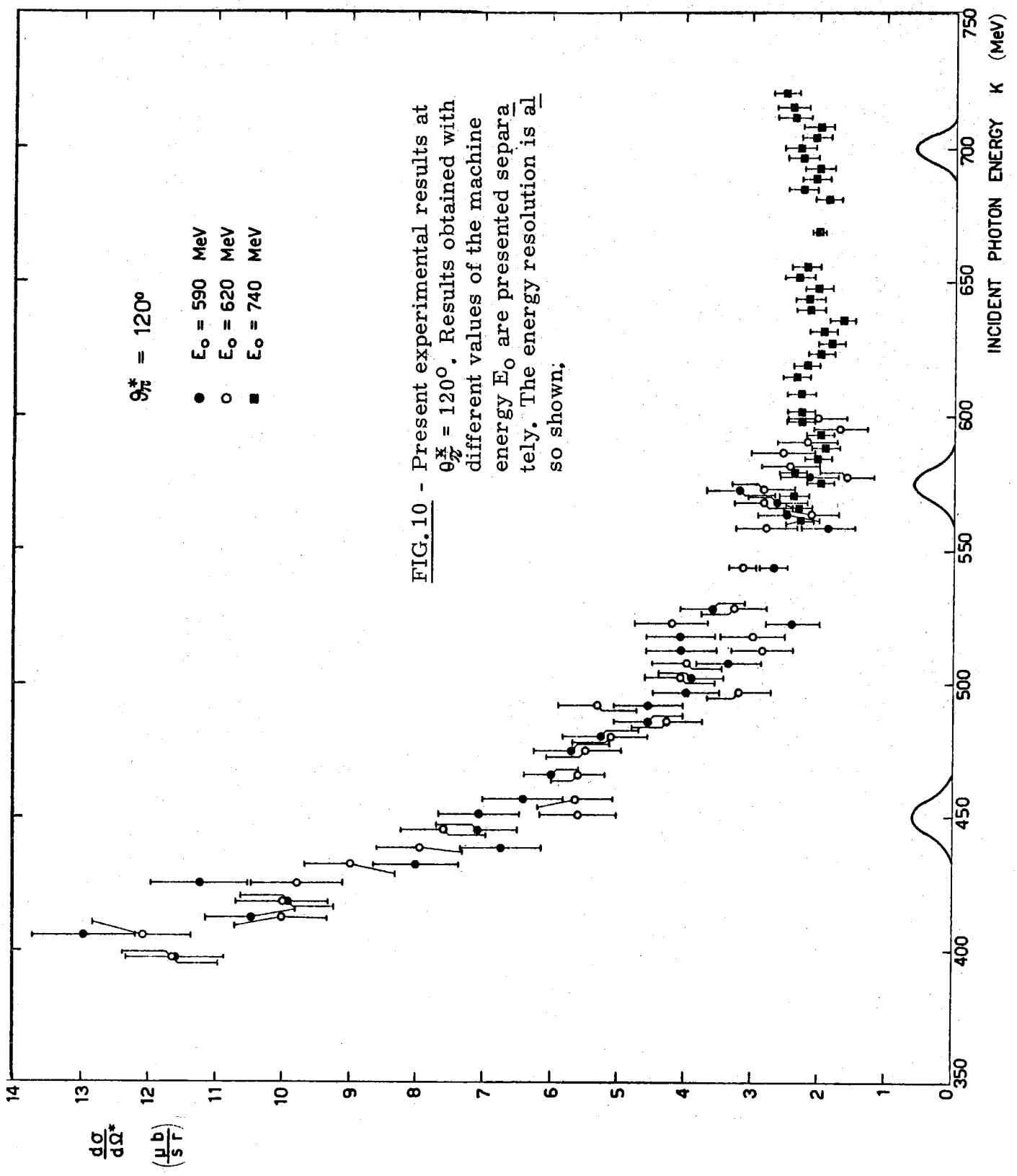

FIG. 10 - Present experimental results at θ^*_π = 120°. Results obtained with different values of the machine energy E_o are presented separately. The energy resolution is also shown;

The kinematical regions covered by our results are shown in fig. 15, from which one can see that our c. m. angular resolution is $\pm$ 5%.

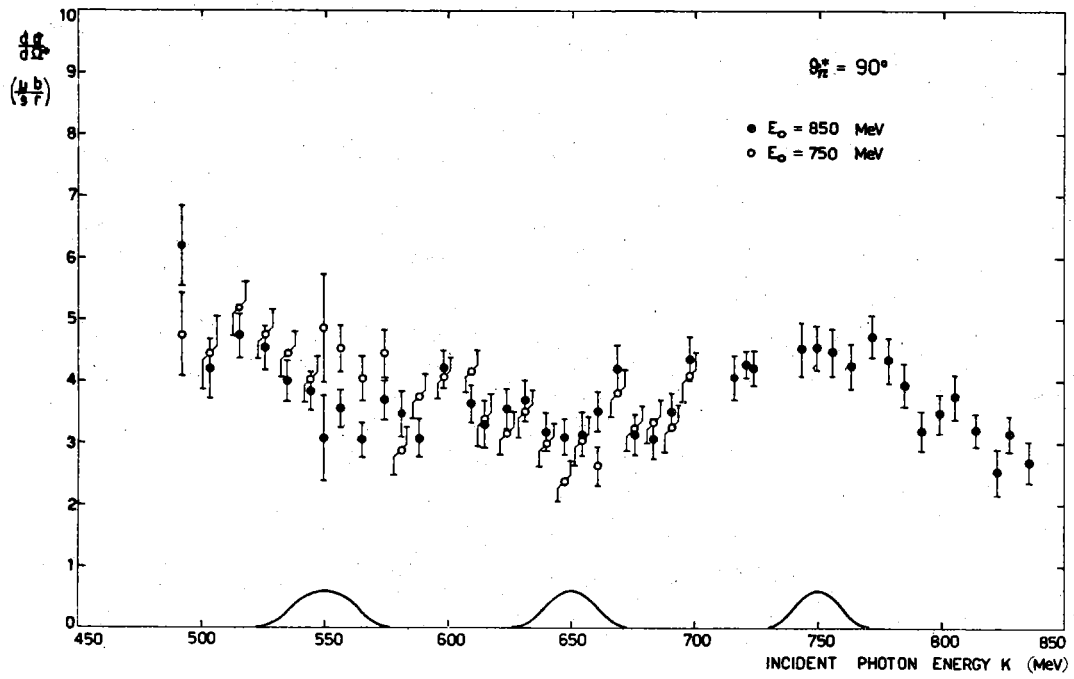

FIG. 11 - Present experimental results at $\theta^*_\pi = 90^\circ$. The results of the two measurement performed at E_o = 850 Mev and E_o = = 750 Mev are presented separately. The energy resolution is also shown.

5) - DISCUSSION OF OUR RESULTS -

The consistency of our results with those available up to now (with lower resolution), is rather good. For a comparison, we have reported in fig. 13 ($\theta^*_\pi = 120^\circ$) along with our results, the results of the experiments available up to now in which both proton and γ were detected in coincidence[9, 10]. No coincidence experiment was available untill now at 135°. The results of previous coincidence experiments at 90° are shown(x) in fig. 14. The single-branch experiments (without detection of the π^o), give in their complex similar results, apart from the fact that they are generally somewhat higher.

For 600 Mev $\lesssim$ k $\lesssim$ 700 Mev, our data at 120° are somewhat lower than the results of other experiments. We have no definite explanation

(x) - To make in fig. 14 clear enough, we were compelled to omit the results of some old experiments; complete references can be found, for instance, in R. Diebold, Phys. Rev. 130, 1089 (1963).

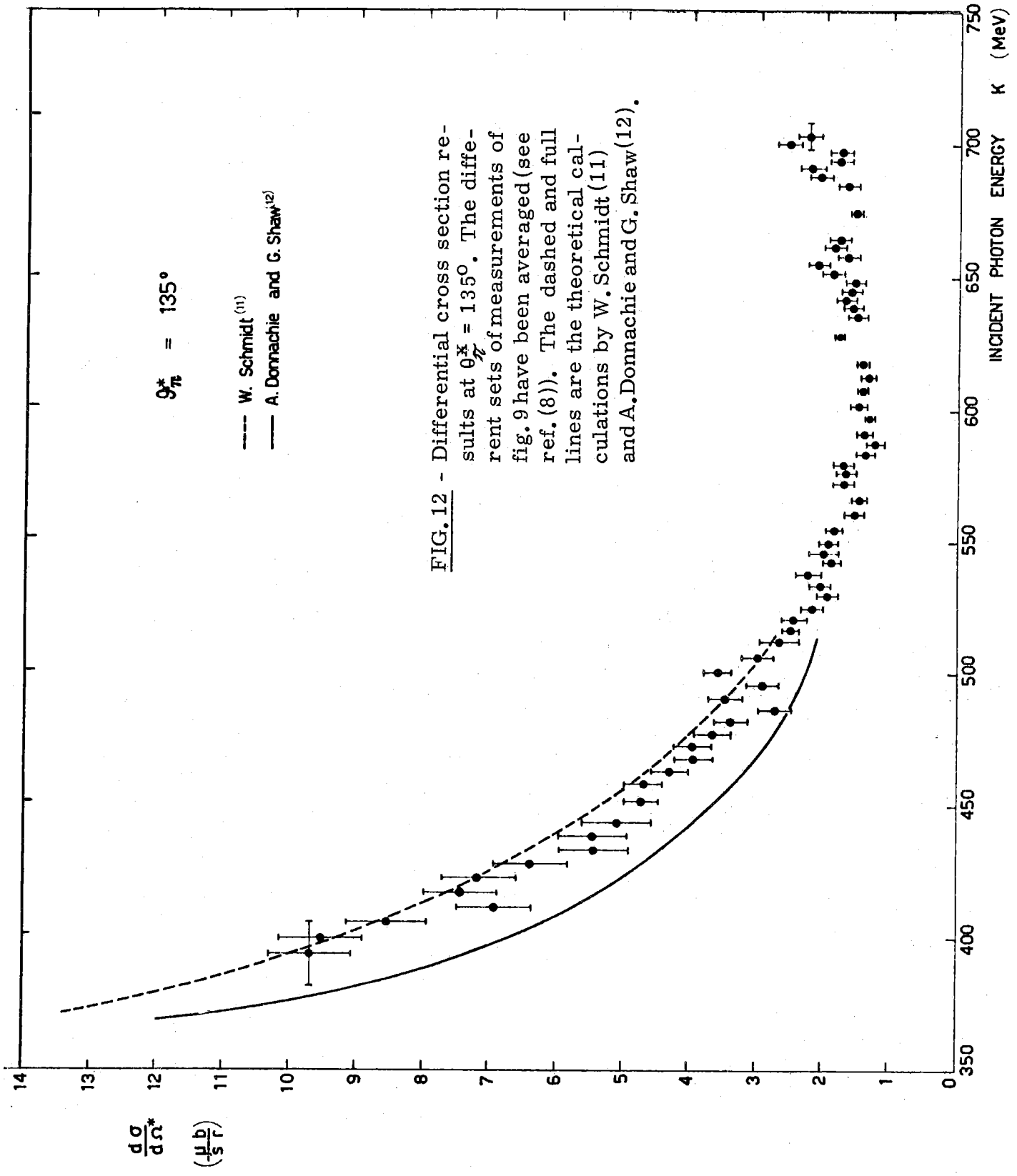

FIG. 12 - Differential cross section results at θ^*_π = 135°. The different sets of measurements of fig. 9 have been averaged (see ref. (8)). The dashed and full lines are the theoretical calculations by W. Schmidt (11) and A. Donnachie and G. Shaw (12).

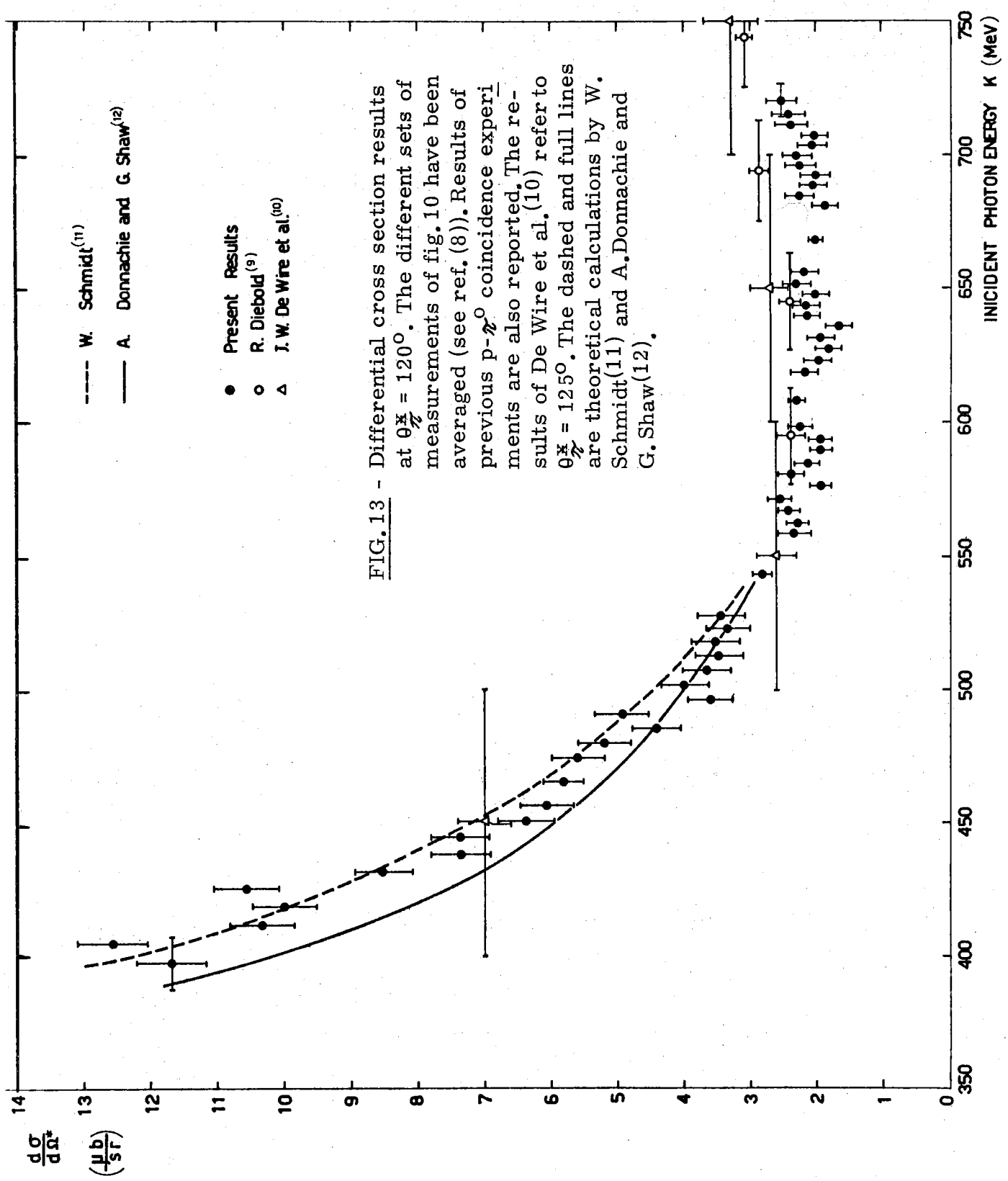

FIG. 13 - Differential cross section results at $\theta^*_{\pi^0} = 120^\circ$. The different sets of measurements of fig. 10 have been averaged (see ref. (8)). Results of previous p-π^0 coincidence experiments are also reported. The results of De Wire et al.(10) refer to $\theta^*_{\pi^0} = 125^\circ$. The dashed and full lines are theoretical calculations by W. Schmidt(11) and A. Donnachie and G. Shaw(12).

for this effect. An over estimate of the mean free path for nuclear absorbtion of protons in the telescope would give an effect in this direction (see Appendix I).

For the following phenomenological discussion of our data, it is convenient to divide the energy interval we explored (400 ÷ 800 Mev) into two parts. The first refers to energies $400 \lesssim k \lesssim 500$ Mev: this part has been treated quite thoroughly with theoretical approaches and multipole analysis[11, 12]. Beyond 550 Mev the situation cannot yet be described in terms of a definite set of multipoles and final states, due to the still insufficient experimental information. We shall therefore analyze our results in terms of a comparison with the results of other reaction channels. The experimental facts which we shall take into account are mainly the increasing evidence of a P_{11} π-N resonance and the photoproduction of the η particle.

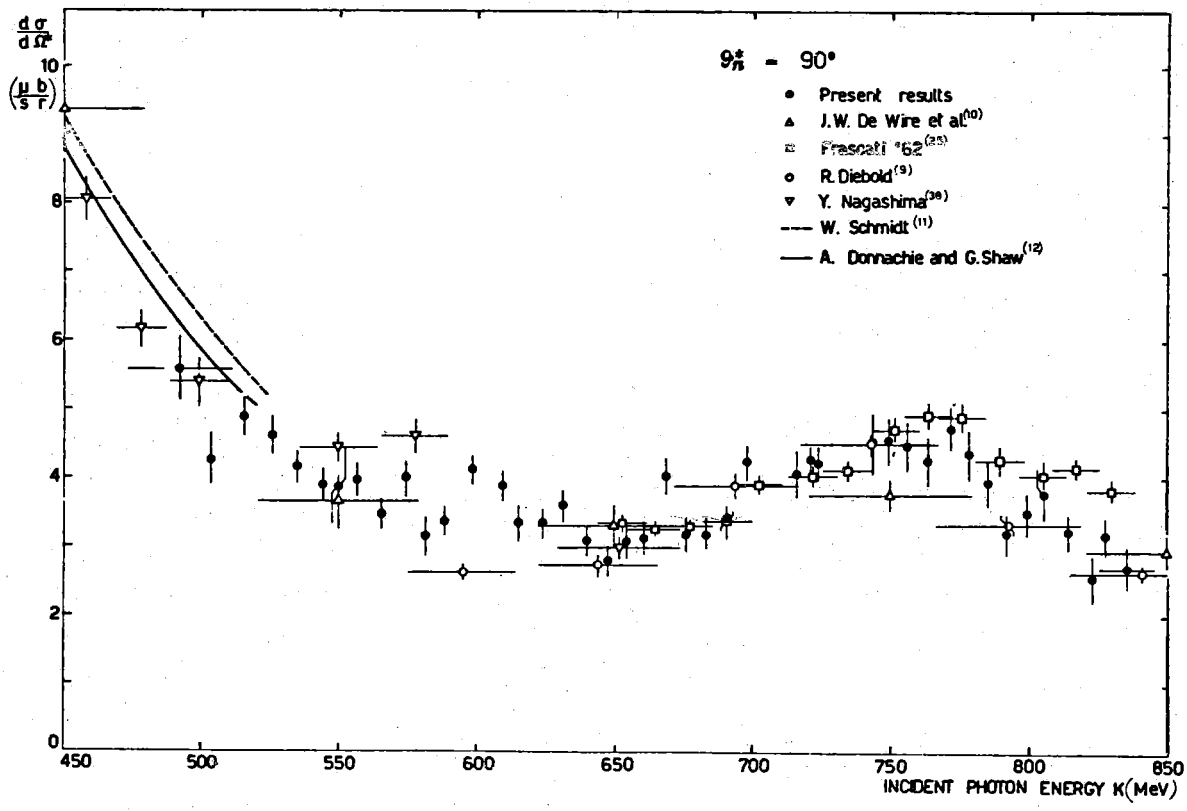

FIG. 14 - Differential cross section results at $\vartheta^*_\pi = 90^\circ$. The different sets of measurements of fig. 11 have been averaged (see ref. (8)). Results of previous p-π^0 coincidence experiments are also reported(+). The dashed and full lines are theoretical calculations by W. Schmidt[11] and A. Donnachie and G. Shaw[12].

For $k \lesssim 550$ Mev, the agreement of our results with the available theoretical predictions (full and dashed lines of figs. 12, 13 and 14) is considerably good. The models used by W. Schmidt[11] and A. Donnachie et al.[12] to make their predictions, are based on the use of the fixed t dispersion rela

tions: since, in addition to other approximations, they neglect in the integrals the imaginary part of the M_{1-} multipole (responsible of the P_{11} state) and of the higher multipoles, it is remarkable that they find such a good fit to the experimental points. Perhaps an upper limit for the amplitude of this "resonating" M_{1-} multipole could be calculated.

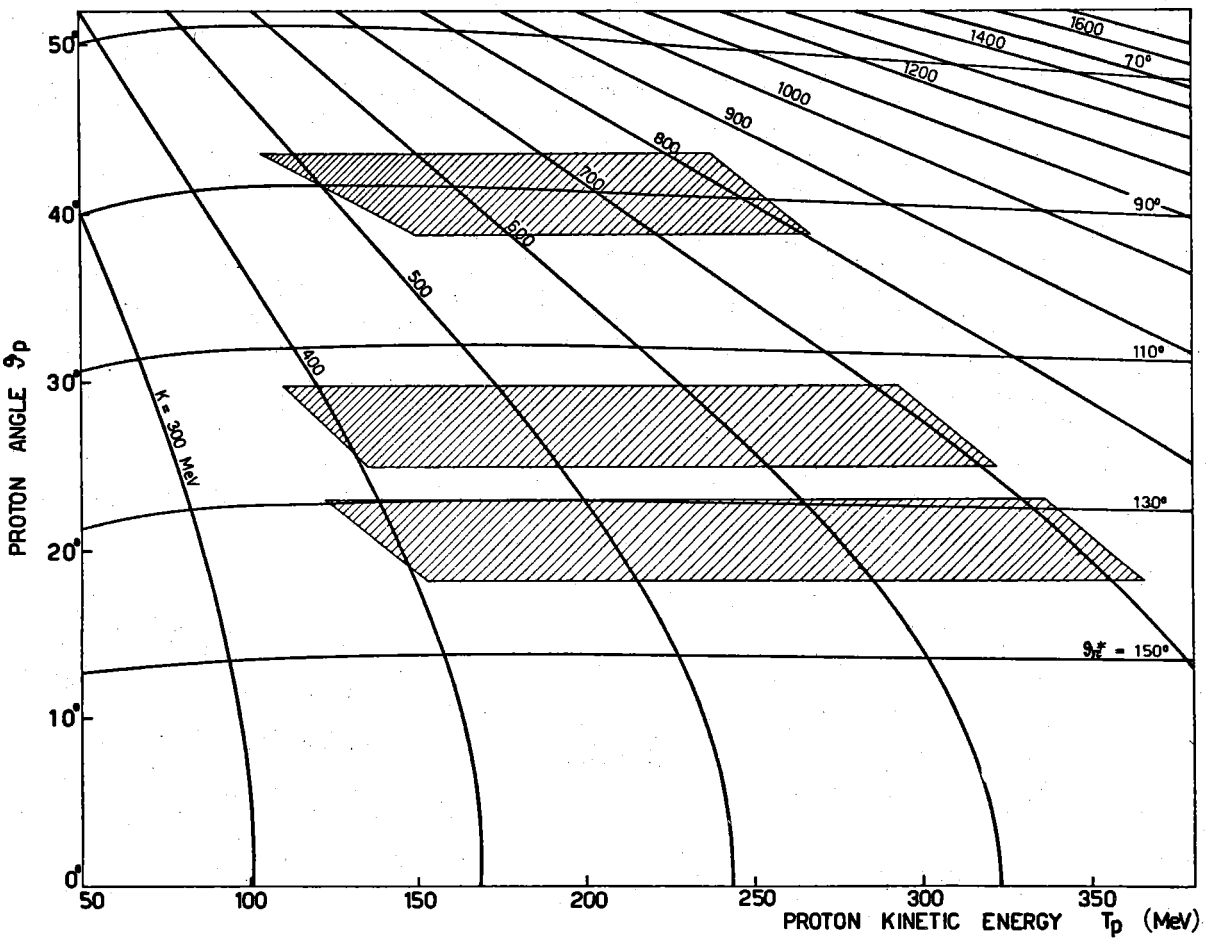

FIG. 15 - Kinematical regions covered by the measurements performed in the present experiment.

Looking now at the energy interval from 550 Mev to 650 Mev, we first observe that our cross sections do not exhibit any evident bump or anomaly while descending from the first resonance towards a significant minimum between 600 Mev and 650 Mev, and rising again towards a maximum which is usually considered as the "second resonance" or D_{13} state. This behaviour is similar to what observed at smaller angles[13]. We recall that in this energy region the P_{11} "resonance" is expected to show up. However, the position and nature of this "resonance" is not yet established. It was observed as a bump in the π-N cross section or in a π-N invariant mass spectrum[15, 15, 16] at $\sim$ 1410 Mev. Phase shifts analyses have confirmed the importance of the P_{11} state: some of these support the hypothesis of a

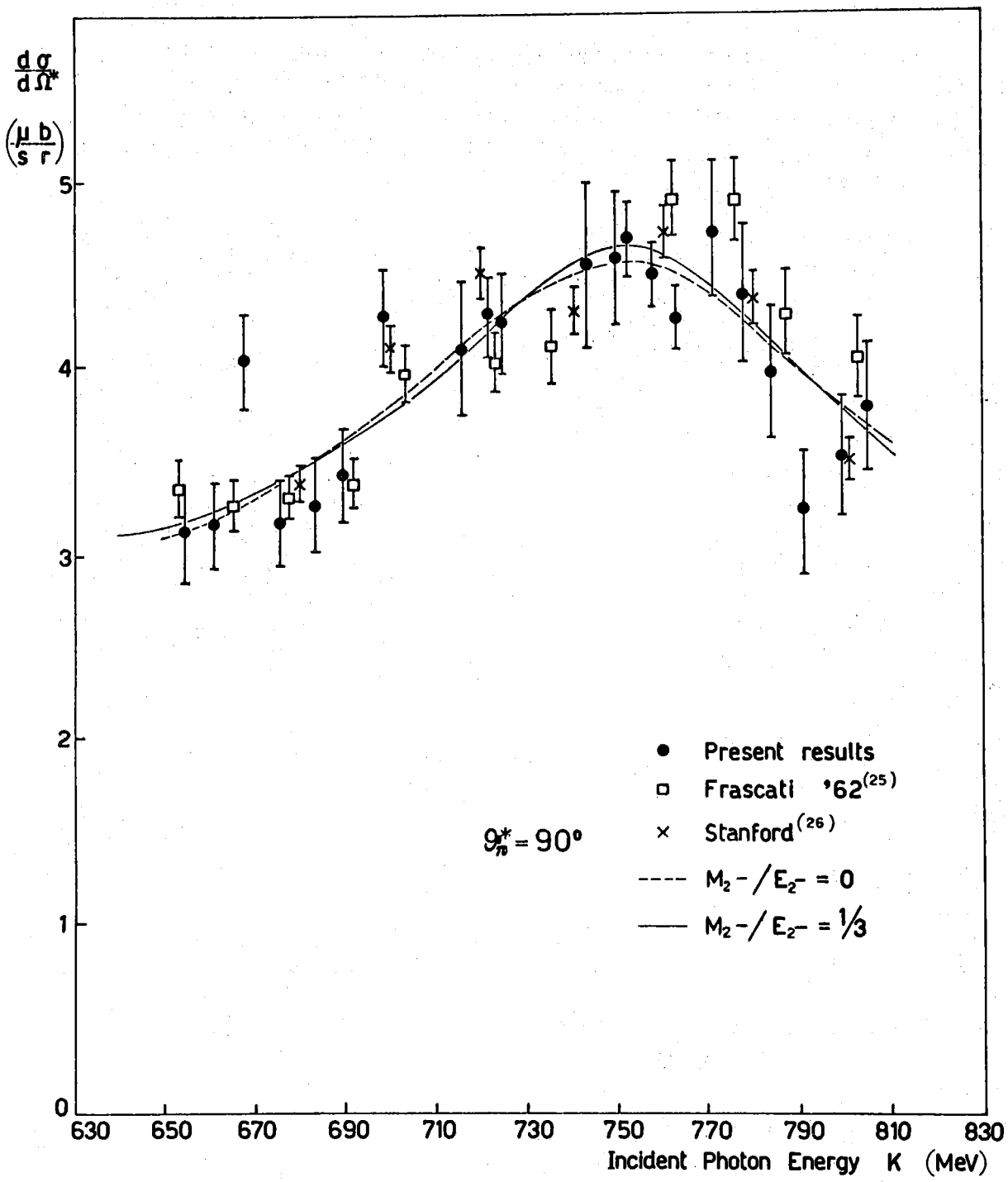

FIG. 16 - The differential cross section for π^0 photoproduction at $\theta^*_\pi = 90^0$, in the energy interval 650 ÷ 810 Mev, as obtained in three experiments performed with good energy resolution. The curves are best fits of the 90^0 differential cross section for π^0 photoproduction, assuming for the η-nucleon system an S_{11} resonant state at the threshold. The resonant part of the second resonance multipoles M_{2-}, E_{2-} has been taken of the Breit-Wigner type (see Appendix II).

resonance (essentially anelastic), giving however in general an higher value for its mass: 1425 Mev[17]; 1485 Mev[18]; 1510 Mev[19,20,21,22]. In other analyses, a phenomenological interpretation of the π-N interaction is given, not requiring the P_{11} state to resonate[23,24]. Also the width of this "resonance" is not established, going from ~60 Mev to ~250 Mev according to the different authors.

We stress that the fact that we do not observe any bump below $E^* = 1450$ Mev, cannot be considered as an evidence against the presence of a P_{11} resonance in our channel: a very broad bump, as the P_{11} resonance is expected to show up, could in fact be masked between the tails of the first and second resonance.

In addition, one should remember that in photoproduction both an isoscalar and an isovector part contribute to each multipole. It may happen that those two contributions are of the same order but opposite in sign for the P_{11} resonance, so that the two contributions cancel each other.

If this is the case, the P_{11} resonance should be important in the photoproduction of pions on neutrons. The relative sign of the isoscalar and isovector contributions is in fact opposite when the photoproduction occurs on neutrons instead than on protons(x).

We now look beyond k = 650 Mev. We have collected data in this energy only at 90°. In fact, at $\theta^*_\pi = 120°$ and 135°, the nuclear absorption of protons does not allow to extend the measurements up to this energy interval using a range telescope. In fig. 16 (and table IV) we show, together with our results, the results of the two other experiments[25,26] performed with a good energy resolution. All of them show a fast rise of the cross section at ~700 Mev followed by a flat region, and another rise around 740 Mev. This anomaly is not significant enough in each experiment considered separately, but may become significant as the results are considered together. Of course, this anomaly could even be the manifestation of the P_{11} resonance in photoproduction; however, its width seems to be too small and its position too high with respect to what is observed in other reaction channels (ref. 14, 15, 16).

Considering that 710 Mev is just the threshold for η photoproduction, we tried to interprete the observed anomaly also through a different mechanism, i.e. as a cusp effect due to the sharp opening of the η-photoproduction channel; this mechanism was first predicted by Rekalo[27] for π^0 photoproduction. In the following we develop somewhat this point.

The following facts[1] should be kept in mind:

(x) - We thank Prof. W. Schmidt for emphasizing this point to us.

a) - The π^0 photoproduction seems to occur, in this energy region, mainly in a T = 1/2 isospin state, as the photoproduction of η's.

b) - The η photoproduction cross section has a very fast rise near threshold[39].

An exact calculation of the η cusp effect is not possible, due to the present lack of knowledge of the multipoles which are important in photoproduction in the region of the second resonance. We have however tried a calculation in a simplified model (some details are given in appendix II), standing on a few basic assumptions which we outline in the following:

1) - According to the results of ref. (28) we assume that the η is produced near threshold in an S_{11} state. The η cusp effect should then reflect, in π^0 photoproduction, on the E_{0+} dipole.

2) - We neglect the multipion production, as the behaviour of the inelasticity parameter in the S_{11} state seems to suggest[19, 20]. Thus, we apply the unitarity and time-reversal invariance of the S matrix, disregarding all reactions but:

$$\pi N \longrightarrow \pi N;\quad \pi N \longrightarrow \eta N;\quad \gamma N \longrightarrow \pi N;\quad \gamma N \longrightarrow \eta N;\quad \eta N \longrightarrow \eta N$$

A set of equations is obtained, which have an unique solution[29] if we further assume that the η-N system is produced through a resonating state, in both input channels π+p and γ+p; again according to ref. (28), we have assumed that the S_{11} η-N resonance occurs at E^{x} = 1520 Mev.

In this way, the $E_{0+}(T = 1/2)$ multipole[(x)] can be determined in terms of measured quantities, i.e. the S_{11} π-N scattering amplitude and the η photoproduction cross section. Informations on the others multipoles necessary to build up the overall π^0 photoproduction cross section have been extracted mainly from ref. (11) and (12). The explicit expression of the cross section is given in Appendix II. In fig. 16 the best fits we could obtain in the two cases $M_{2-}/E_{2-} \simeq 0$[30] or $M_{2-}/E_{2-} \simeq 1/3$[31] are compared with the experimental results. As we see, the computed curves do not fit the anomaly observed at $E \simeq 700 \div 740$ Mev: the perturbation due to the η-channel remains small, notwithstanding the sharp rise of the η-photoproduction cross section.

Apart from the doubts one could have, that the observed anomaly is a fluctuation, the reason of the discrepancy could be found in the initial assumption of an S_{11} η-N resonant state, as well as in our approxima

---

(x) - Here and in the following we use for the multipoles standard notations (E_{e+}; M_{e+} are defined, for instance, in G. F. Chew, M. L. Goldberger, F. E. Low and Y. Nambu, Phys. Rev. 106, 1345 (1957)).

tions in calculating the anomaly. It is worthwile to remember that the η-N system could even be in a different state, other than the S_{11}, and therefore the overall situation could be more complicated. In particular a P_{11} resonant state with even large interferences with other states, cannot be excluded. Of course in this case the two independent searches we did in this part of our paper, that is for some evidence of the P_{11} resonance, and for the η cusp effect, could even coincide. Some further remarks on this point are given in Appendix II.

In addition, as recently pointed out by several authors[32,33,34], also the D_{13} state could be important in the η photoproduction, in which case a naive approach could be even more inadeguate.

6) - CONCLUSIONS -

We summarize our results and discussion in the following points:

1) - Measurements of the π^o photoproduction cross section have been performed by us with good energy resolution.

2) - The π^o photoproduction cross section seems to be well described by the theoretical calculations based on dispersion relations[11, 12] up to k = 550 Mev of the incident photon (E^* = 1380 Mev total energy in the center of mass system).

3) - We do not see any significant evidence of a new isobaric state, like the P_{11}, state observed in many experiments[14, 15, 16] and in phase shifts analysis[17 ÷ 22], at c.m. total energies smaller than 1480 Mev.

4) - There is an experimental indication (see fig. 16) of a possible structure in the region of the second resonance at k = 700 ÷ 740 Mev. We tried to interprete it as an η cusp effect. A rough estimate, assuming that the η is produced near threshold in a S_{11} resonant state, predicts an anomaly much smaller that the observed one. A possible reason of this discrepancy could be that the η-N system is at the threshold in a different state, other than S_{11} state. In particular a P_{11} resonant state with interferences with other states, cannot be excluded according to the experimental information available up to now.

Thanks are due to Prof. W. Schmidt for valuable critical remarks and suggestions.

We wish to thank our technicians V. Bidoli, I. Bruno and M. Massimi for their helpful assistance in setting up the apparatus and mantaining it during its long operation. The skillness and patience of the scanners Mrs. and Mr. Melorio and Mr. E. Paganelli is also acknowledged. Finally, we wish to thank the synchrotron staff, for their collaboration during our runs.

APPENDIX I -

In addition to the statistical errors, quoted in figs. 12, 13, 14 and in Tables I, II and III, other kinds of errors do affect our results.

However, since all these errors, but the statistical ones, are constant or have a smooth behaviour as a function of energy, our discussion of par. 5, in which the absolute normalization was not of relevant importance, was based on the results affected by the statistical errors only.

The most important sources of errors we could think of, in addition to statistics, are the following:

1) - Calibration of the Wilson quantameter. We believe to our quantameter to within $\pm$ 5%. An error in its calibration would affect our results for a constant factor, independent of energy.

2) - π^0's not detected by C due to the electronics threshold. By extrapolating below threshold the pulse height distributions in C (fig. 7), we have evaluated this correction as being:

for $\theta_\pi^* = 135^\circ$ 10% at k = 400 Mev, going smoothly to 4% at $k \simeq 700$ Mev

for $\theta_\pi^* = 120^\circ$ 10% at k = 400 Mev, going smoothly to 4% at $k \simeq 700$ Mev

for $\theta_\pi^* = 90^\circ$ 5% at k = 550 Mev, going smoothly to zero at $k \simeq 850$ Mev

Our evaluation of the error in this correction is $\pm$ 60% of the correction itself.

3) - Nuclear interactions. We have used a mean free path for nuclear interactions of protons in Aluminum λ = 110 gr/cm^2. This value of λ is affected by an error, since it is extracted from the results of an experiment[5] performed in a different geometrical situation than ours. We have elaborated our results also using for λ the values of 80 gr/cm^2 and 140 gr/cm^2; this is in our opinion the maximum range of values for λ in our conditions. The results are summarized in table A1. As one can see, using a value of λ of 95-100 gr/cm^2 would bring our points at higher energy ($\theta_\pi^* = 120^\circ$) into agreement with previous results, leaving unaffected the agreement of the other points (at the three angles).

APPENDIX II -

We report here some details on the calculation performed to estimate the η cusp effect. A full account can be found in ref. (29).

Assuming that only the multipoles E_{o+}, M_{1+}, E_{2-}, M_{2-} are important in the region of the second resonance, the 90° differential cross section for reaction (1) can be written:

$$\frac{K}{q}\left(\frac{d\sigma}{d\Omega^{x}}\right) = \left|E_{o+}\right|^2 + \frac{5}{2}\left|M_{1+}\right|^2 + \frac{5}{2}\left|E_{2-}\right|^2 + \frac{9}{2}\left|M_{2-}\right|^2 - \mathrm{Re}\, E^{x}_{o+}(E_{2-} - 3M_{2-}) + \tag{A1}$$

$$+ 3\,\mathrm{Re}\, M^{x}_{2-}\, E_{2-}$$

where K and q are the c.m. momentam of the photon and meson respectively.

The E_{o+} multipole has been evaluated under the assumptions listed in par. 5. Let's write it in the form

$$E_{o+} = \frac{2}{3} E^{3/2}_{o+} + \frac{1}{3} C e^{i\gamma_o} .$$

The $E^{3/2}_{o+}$ part which is not expected to change very fast in our energy region, has been extrapolated from ref. (11, 12); C and γ_o were determined from the amplitudes of π's and η's photo and pi-production, using the unitarity and time reversal invariance of the S-matrix.

The first resonance multipole M_{1+} has been taken from ref. (11, 12).

Concerning the ratio $r = M_{2-}/E_{2-}$ of the magnetic to the electric T = 1/2 amplitude, we considered both the cases $r \simeq 0$ (case a) and $r \simeq$ $\simeq 1/3$ (case b). The first case is suggested by ref. (30); the second one is even more firmly supported by theoretical analyses(31, 35) which need an 1/3 ratio to explain the experimental results on the forward π^o photoproduction cross section(37). The T = 3/2 non resonating part of the E_{2-} multipole has been taken from ref. (11, 12). For the resonating T = 1/2 part of this multipole we assumed a Breit-Wigner (BW) shape:

$$-\frac{B\Gamma E_{res}}{(E^2 - E^2_{res}) + i\Gamma E_{res}}$$

The amplitude B and the width Γ are free parameters to be determined by best fitting with (A. 1) the experimental results in the energy region 650 ÷ ÷ 800 Mev (fig. 16 and table A. I).

The resonance energy was E_{res} = 1518 Mev, as suggested in ref. (20).

However this fit gives always a rather bad agreement. To improve the best-fit, we tried to take into account a background from the previously neglected multipoles and their interference with the BW or E_{o+} terms. Only the real parts have been considered.

Therefore the additional quantity:

$$\alpha \text{ Re (BW)} + \beta \text{ Re } E_{o+} + \gamma$$

was added to (A. 1); α , β , γ are real energy independent coefficients, which stand for rather cumbersome combinations of those smaller multipoles.

The best-fit obtained by varying B, Γ, α , β , γ are shown in fig. 16. The resulting sets of important parameters are:

case a) - (r=0), χ^2 = 72 (33 deg. of freedom); Γ = 80 Mev; $B/(10^{-2} \lambda\!\!\!^{-}_{\pi}) = 0.8$

case b) - (r=1/3), χ^2 = 73 (33 deg. of freedom); Γ = 80 Mev; $B/10^{-2} \lambda\!\!\!^{-}_{\pi}) = 0.5$

We didn't to get some better fit because this result would be achieved by increasing the number of independent parameters, but then all the procedure would loose in information. In conclusion the variation of the E_{o+} multipole as a function of the energy, going through the η threshold, is not great enough to explain the observed anomaly. Unless a more refined treatment shows that this anomaly comes out from a complicated interference of all the multipoles which are present, one could try to calculate the cusp effect on some different assumption.

For instance, one could assume for the η-N system a P_{11} wave bound state. This possibility cannot be excluded by the present experimental evidence. In fact the assignement of the orbital angular momentum of the η-N system was mainly based on the fact that the S_{11} wave, in π-N scattering, shows an anelasticity parameter changing abruptly from 1 just at the opening of the η production channel. However, mainly according to ref. (23), also the P_{11} anelasticity parameter changes enough to allow the opening of the η production channel. Further informations can be obtained by an analysis of the η production cross section as a function of the energy just near threshold.

On this lines, some authors[36] are in favour of an S_{11} state; however we have tried a similar analysis, and found that both the hypotheses of an S_{11} state η-N real resonance and of a P_{11} wave bound state below threshold are consistent.

TABLE I

Differential cross sections in the c. m. for the process $\gamma + p \rightarrow \pi^o + p$
Experimental results at $\theta^x = 135^o$ vs. the energy k of the incident photon.

k (MeV)	$d\sigma/d\Omega^x$ (μb/sr)	k (MeV)	$d\sigma/d\Omega^x$ (μb/sr)
394	9.68 ± 0.62	561	1.53 ± 0.14
400	9.53 ± 0.62	566	1.45 ± 0.13
406	8.53 ± 0.60	572	1.68 ± 0.16
411	6.90 ± 0.56	576	1.65 ± 0.15
417	7.39 ± 0.57	580	1.69 ± 0.16
422	7.16 ± 0.57	584	1.37 ± 0.14
428	6.37 ± 0.55	587	1.22 ± 0.14
433	5.42 ± 0.52	591	1.39 ± 0.11
438	5.45 ± 0.52	597	1.31 ± 0.06
444	5.07 ± 0.51	602	1.47 ± 0.12
452	4.71 ± 0.25	608	1.41 ± 0.08
458	4.67 ± 0.28	613	1.32 ± 0.10
463	4.28 ± 0.28	618	1.41 ± 0.08
468	3.93 ± 0.27	628	1.76 ± 0.06
472	3.94 ± 0.27	636	1.47 ± 0.13
477	3.64 ± 0.26	640	1.57 ± 0.14
482	3.37 ± 0.26	643	1.66 ± 0.14
487	2.70 ± 0.23	646	1.58 ± 0.14
491	3.45 ± 0.26	649	1.51 ± 0.14
495	2.89 ± 0.24	653	1.86 ± 0.15
501	3.56 ± 0.21	656	2.08 ± 0.16
506	2.96 ± 0.25	659	1.61 ± 0.14
512	2.65 ± 0.29	662	1.82 ± 0.15
517	2.47 ± 0.12	666	1.75 ± 0.15
521	2.43 ± 0.17	676	1.53 ± 0.06
525	2.15 ± 0.16	686	1.64 ± 0.15
530	1.93 ± 0.15	689	2.06 ± 0.16
534	2.03 ± 0.15	692	2.20 ± 0.17
538	2.22 ± 0.16	695	1.77 ± 0.16
542	1.86 ± 0.12	698	1.75 ± 0.16
546	1.98 ± 0.22	701	2.52 ± 0.19
549	1.90 ± 0.15	704	2.22 ± 0.18
555	1.83 ± 0.13		

TABLE II

Differential cross sections in the c. m. for the process $\gamma + p \rightarrow \pi^0 + p$
Experimental results at $\theta^{*}_{\pi^0} = 120^0$ vs. the energy k of the incident photon.

k (MeV)	$d\sigma/d\Omega^{*}$ (μb/sr)	k (MeV)	$d\sigma/d\Omega^{*}$ (μb/sr)
397	11,68 ± 0,51	580	2.41 ± 0.18
404	12.57 ± 0,53	585	2,15 ± 0.18
411	10.33 ± 0,49	589	1.96 ± 0.17
418	9.99 ± 0,48	594	1.95 ± 0.17
425	10.57 ± 0,50	598	2.27 ± 0.18
431	8.52 ± 0,46	608	2.32 ± 0.12
438	7.35 ± 0,43	619	2.20 ± 0.21
444	7.37 ± 0,44	623	2.00 ± 0.20
450	6.38 ± 0,42	627	1.84 ± 0.19
456	6.06 ± 0,41	631	1.97 ± 0.20
465	5,82 ± 0,29	636	1.68 ± 0.19
474	5,61 ± 0,40	640	2,16 ± 0.21
480	5,21 ± 0,40	644	2,18 ± 0.21
486	4,43 ± 0,37	648	2,04 ± 0.20
491	4,94 ± 0,39	652	2,33 ± 0.22
496	3,62 ± 0,35	656	2,22 ± 0.21
502	4,01 ± 0,36	668	2,04 ± 0,09
507	3,67 ± 0,35	681	1,90 ± 0.20
512	3,48 ± 0,34	685	2,28 ± 0.22
517	3,54 ± 8,35	688	2,08 ± 0.21
523	3,35 ± 0,34	692	2,03 ± 0.21
528	3,46 ± 0,35	696	2,28 ± 0,23
543	2,84 ± 0,14	700	2,33 ± 0.23
558	2,36 ± 0,25	704	2,09 ± 0.22
562	2,32 ± 0,17	707	2,06 ± 0.22
667	2,45 ± 0,17	711	2,41 ± 0.24
572	2,57 ± 0,18	715	2,44 ± 0.25
576	1,97 ± 0,16	720	2,55 ± 0.18

TABLE III

Differential cross sections in the c. m. for the process $\gamma + p \rightarrow \pi^0 + p$. Experimental results at $\theta^{*}_{\pi^0} = 90^{\circ}$ vs. the energy k of the incident photon.

k (MeV)	$d\sigma/d\Omega^{*}$ (μb/sr)	k (MeV)	$d\sigma/d\Omega^{*}$ (μb/sr)
491	5.62 ± 0.47	668	4.04 ± 0.26
503	4.31 ± 0.38	676	3.19 ± 0.23
515	4.94 ± 0.28	683	3.19 ± 0.24
525	4.63 ± 0.27	691	3.40 ± 0.24
534	4.20 ± 0.24	698	4.25 ± 0.27
544	3.92 ± 0.23	716	4.06 ± 0.36
549	3.91 ± 0.55	721	4.26 ± 0.22
556	3.98 ± 0.24	724	4.22 ± 0.27
565	3.50 ± 0.23	743	4.53 ± 0.44
574	4.02 ± 0.24	749	4.56 ± 0.36
581	3.19 ± 0.27	756	4.48 ± 0.36
588	3.39 ± 0.23	763	4.25 ± 0.36
598	4.15 ± 0.22	772	4.73 ± 0.35
609	3.88 ± 0.23	778	4.38 ± 0.37
614	3.34 ± 0.28	784	3.96 ± 0.36
624	3.39 ± 0.24	791	3.21 ± 0.33
631	3.61 ± 0.24	799	3.50 ± 0.31
639	3.10 ± 0.23	805	3.77 ± 0.36
647	2.81 ± 0.22	814	3.22 ± 0.27
654	3.10 ± 0.27	822	2.55 ± 0.36
661	3.15 ± 0.23	827	3.17 ± 0.31
		835	2.71 ± 0.33

TABLE IV

Differential cross section in the c. m. for the process $\gamma + p \rightarrow \pi^o + p$ at $\theta_\pi^* = 90^o$ vs. the energy k of the incident photon (fig. 16); experiments performed with good energy resolution: (a) present results; (b) Frascati 1962[25]; (c) Stanford[26].

k (MeV)	$d\sigma/d\Omega^*$ (μb/sr)	Ref.	k (MeV)	$d\sigma/d\Omega^*$ (μb/sr)	Ref.
653	3.34 ± 0.15	b	784	3.96 ± 0.36	a
654	3.10 ± 0.27	a	789	4.26 ± 0.23	b
661	3.15 ± 0.23	a	791	3.21 ± 0.33	a
665	3.25 ± 0.13	b	799	3.50 ± 0.31	a
668	4.04 ± 0.26	a	800	3.50 ± 0.10	c
676	3.19 ± 0.23	a	804	4.04 ± 0.21	b
678	3.30 ± 0.11	b	805	3.77 ± 0.36	a
680	3.37 ± 0.11	c			
683	3.19 ± 0.24	a			
691	3.40 ± 0.24	a			
692	3.37 ± 0.13	b			
698	4.25 ± 0.27	a			
700	4.09 ± 0.12	c			
703	3.96 ± 0.15	b			
716	4.06 ± 0.36	a			
720	4.48 ± 0.13	c			
720	4.02 ± 0.15	b			
721	4.26 ± 0.22	a			
724	4.22 ± 0.27	a			
736	4.10 ± 0.20	b			
740	4.29 ± 0.13	c			
743	4.53 ± 0.44	a			
749	4.56 ± 0.36	a			
753	4.67 ± 0.20	b			
756	4.48 ± 0.36	a			
760	4.70 ± 0.14	c			
762	4.88 ± 0.20	b			
763	4.25 ± 0.36	a			
772	4.73 ± 0.35	a			
776	4.87 ± 0.21	b			
778	4.38 ± 0.37	a			
780	4.35 ± 0.13	c			

TABLE A.I

Effect of a possible error in λ on our results. For instance at 135°, increasing λ of 27% (from λ = 110 to λ = 140 gr/cm^2) would decrease the cross section of an amount which goes smoothly from 1.8% at k = 400 Mev, to 4.5% at k = 500 Mev, etc.

θ_π^*	$\delta\lambda$	$\Delta\sigma/\sigma$	$\Delta\sigma/\sigma$	$\Delta\sigma/\sigma$	$\Delta\sigma/\sigma$
		at k = 400	at k = 500	at k = 600	at k = 700
135°	+27%	-1.8%	-4.5%	-5.5%	-12.5%
	-27%	+3.8%	+8.2%	+10.0%	+27.9%
	~~+27%~~	at k = 400	at k = 500	at k = 600	at k = 700
120°	+27%	-1.8%	-3.3%	-4.2%	-10.4%
	-27%	+2.0%	+5.9%	+7.1%	+21.1%
		at k = 525	at k = 680	at k = 820	
90°	+27%	+1.5%	-2.0%	-8.4%	
	-27%	-3.1%	+3.0%	+16.6%	

REFERENCES -

(1) - C. Bacci, G. Penso, G. Salvini, C. Mencuccini and V. Silvestrini, Phys. Rev. Letters 16, 157 (1966); Phys. Rev. Letters 16, 384 (1966); C. Bacci, C. Mencuccini, G. Penso, G. Salvini and V. Silvestrini, LNF-66/20; Nuovo Cimento 45, 983 (1966).
(2) - C. Bacci, C. Mencuccini, G. Penso, V. Silvestrini, M. Spinetti and B. Stella, Rendiconti dell'Accademia dei Lincei 39, 452 (1965).
(3) - V. Montelatici, Nuclear Instr. and Meth. 29, 121 (1964).
(4) - R. R. Wilson, Nuclear Instr. and Meth. 1, 101 (1957).
(5) - G. P. Millburn, N. Birnbaum, W. E. Crandall and L. Schecter, Phys. Rev. 95, 1268 (1954).
(6) - R. F. Stiening, E. Loth and M. Deutsch, Phys. Rev. Letters 10, 536 (1963).
(7) - D. R. Rust, E. Eisenhandler, P. J. Mostek, A. Silverman, C. K. Sinclair and R. M. Talman, Phys. Rev. Letters 15, 938 (1965).
(8) - F. S. Crawford Jr., Nuclear Instr. and Meth. 33, 332 (1965).
(9) - R. Diebold, Phys. Rev. 130, 2089 (1963).
(10) - J. M. DeWire, H. E. Jackson and R. Littauer, Phys. Rev. 110, 1208 (1958).
(11) - W. Schmidt, Z. Physik 182, 76 (1964).
(12) - A. Donnachie and G. Shaw, Photopion production, dispersion relations and γ - ϱ - π coupling, to be published in Ann. of Phys.
(13) - G. Bellettini, C. Bemporad, P. J. Biggs, P. L. Braccini, T. Del Prete and L. Foà, Nuovo Cimento 44, 239 (1966).
(14) - P. Bareyre, C. Bricman, G. Valladas, G. Villet, J. Bizard and J. Seguinot, Phys. Letters 8, 137 (1964).
(15) - G. Cocconi, E. Lillethum, J. P. Scanlon, C. A. Stahlbrandt, C. C. Ting, J. Walters and A. M. Wetherell, Phys. Letters 8, 134 (1964); G. Bellettini, G. Cocconi, A. N. Diddens, E. Lillethum, J. P. Scanlon and A. M. Wetherell, Proceedings of Hamburg Int. Conference, (1965), pag. 97; G. Bellettini, G. Cocconi, A. N. Diddens, E. Lillethum, J. P. Scanlon, A. M. Shapiro and A. M. Wetherell, Phys. Letters 18, 167 (1965).
(16) - S. L. Adelman, Phys. Rev. Letters 13, 555 (1964).
(17) - S. L. Adelman, Phys. Rev. Letters 14, 1043 (1965).
(18) - L. D. Roper, Phys. Rev. Letters 12, 340 (1964).
(19) - P. Auvil, C. Lovelace, A. Donnachie and T. A. Lea, Phys. Letters 12, 76 (1964).
(20) - P. Bareyre, C. Bricman, A. V. Stirling and G. Villet, Phys. Letters 18, 342 (1965).
(21) - L. D. Roper, R. M. Wright and B. T. Feld, Phys. Rev. 138, B190 (1965).
(22) - B. H. Bransden, P. J. O'Donnel and R. G. Moorhouse, Phys. Letters 11, 339 (1964).
(23) - J. Cence, Phys. Letters 20, 306 (1966).
(24) - R. H. Dalitz and R. G. Moorhouse, Phys. Letters 14, 159 (1965).

(25) - M. Deutsch, C. Mencuccini, R. Querzoli, G. Salvini, V. Silvestrini and R. Stiening, Proceedings of the Frascati Congress 1962, pag. 28.
(26) - H. De Staebler Jr., E. F. Erickson, A. C. Hearn and C. Schaerf, Phys. Rev. 140, 342 (1965).
(27) - M. P. Rekalo, Soviet Physics JETP 19, 152 (1964).
(28) - A. W. Hendry and R. G. Moorhouse, Phys. Letters 18, 171 (1965).
(29) - C. Mencuccini, A. Reale, to be published.
(30) - Ph. Salin, Nuovo Cimento 28, 1294 (1963).
(31) - D. S. Beder, Nuovo Cimento 33, 94 (1964).
(32) - W. B. Richards, C. B. Chiu, R. D. Eandi, A. C. Helmholz, R. W. Kenney, B. J. Moyer, J. Poirier, R. J. Cence, V. Z. Peterson, N. R. Sehgal and V. J. Stenger, Phys. Rev. Letters 16, 1221 (1966).
(33) - S. Minami, Phys. Rev. 147, 1123 (1966).
(34) - G. Altarelli, F. Buccella and R. Gatto, Nuovo Cimento 35, 331 (1965).
(35) - A. Bietti, Phys. Rev. 142, 1258 (1966).
(36) - F. Uchiyama-Campbell and R. K. Logan, Phys. Rev. 149, 1220 (1966).
(37) - F. Talman, C. Clinesmith, R. Gomez and A. Tollestrup, Phys. Rev. 9, 177 (1963).
(39) - Y. Nagashima, Thesis Report INSJ-81, TH-47 (Unpublished).
(40) - R. Prepost, D. Lundquist and D. Quinn, Proceedings of the International Symposium on Electron and Photon Interactions at High Energies, June 1965.